Proceedings of the Second International Symposium on
Measurement and Control in Robotics (ISMCR '92)
Tsukuba Science City, Japan - November 15-19, 1992

Coupling a Camera and Laser Stripe in Sensor Based Control

G. Motyl*, F. Chaumette**, J. Gallice*

*Laboratoire d'Electronique, U.R.A 830 du CNRS, 63177 Aubière Cedex, France
**IRISA, Campus Universitaire de Beaulieu, 35042 Rennes Cedex, France

Abstract

A real time visual servoing approach is applied to robotics tasks consisting of the end effector positioning with respect to *a priori* known objects. The vision apparatus which is mounted on the wrist of a robot manipulator is constituted by a CCD camera rigidly coupled with laser stripe.

We formalize the problem in terms of *sensor-based control* applied to visual servoing. This approach consists in the modeling of the interaction between the sensor and its environment. In this paper, with the camera-light stripe coupling, we define *interaction matrices* which correspond to positioning tasks with respect to polyhedral and spherical scenes. The feasibility of this approach is demonstrated in simulation and in real experiment corresponding of one industrial task in automotive industry (polyhedral scene case). Both simulation and experimental results are presented showing the robustness and stability of the control scheme.

Keywords : Sensor based control, Visual servoing

1 Introduction

We are interested in the design of control systems which work in closed loop with respect to visual data provided by the coupling of a camera and light stripe mounted on the end effector of a robot.

One of the main problem in computer vision, which limits its use in robotics applications, is the prohibitive time processing occurring for complex images. Using a camera light stripe as sensor allows to simplify image processing [2]: indeed, only the projection of light stripes on the objects of the scene is perceptible by the camera. This simplicity allows to obtain visual data at a rate (in our case the video rate) consistent with the bandwith of the robot controller and to exploit them in a robust control scheme using the visual servoing approach.

The concept of visual servoing originates from efforts to use wrist-mounted visual sensors to produce feedback information to close the loop of a robotics control scheme. The idea is to extract "relevant" image information which will be useful to realize the desired task (mostly a positioning task). The early applications were based on heuristic approaches [1], [7], followed by a formalization in terms of control theory and a classification of the control strategies [9], [11]. Especially, *Position-Based* and *Image-Based* Visual Servoing were defined. While in both schemes the system stability relies on visual information, in the former the control is synthesized in terms of regulation of the end effector position, while in the latter the control is expressed in terms of regulation in the image. The second scheme, which corresponds to the one we develop, has the advantage of avoiding the intermediary step of the 3D estimation of the workpiece with regard to the end-effector: a *target image* is built, corresponding to the desired position of the end-effector with regard to the workpiece, and a robotics control scheme is developed, based directly on image errors measured between the current image and the target image [6] [3] [5].

2 Visual Servo Control

We formalize the problem in terms of *sensor based control* [4] applied to visual servoing. The visual information, provided by the wrist-mounted sensory apparatus, is modeled as a set of *elementary signals* $\underline{s}$ associated to the 2D geometric primitives in the image corresponding to the projection of the 3D primitives in the scene. The interaction between the sensor and the scene is described by a *coupling matrix* $L_{\underline{s}}^T$ which links

PR0003/92/0000-0685

the behavior of the signal to the sensor and/or object motion:

$$\dot{\underline{s}} = L_{\underline{s}}^T . \xi \quad (1)$$

where

- $\dot{\underline{s}}$ is the time variation of $\underline{s}$;
- ξ is the object velocity with respect to the sensor;
- $L_{\underline{s}}^T$, called *interaction matrix* related to $\underline{s}$, corresponds to the jacobian of $\underline{s}$ [5].

A robust control scheme based on the *task function approach* is then derived [8]. For a given task, we have to choose a set $\underline{s}$ of visual features suited for achieving the task. Then, we can define a task function vector $\underline{e}(t)$ such that:

$$\underline{e}(t) = C\ (\underline{s}(t) - \underline{s}^*) \quad (2)$$

where

- $\underline{s}^*$ can be considered as a reference image target to be reached in the image frame;
- $\underline{s}(t)$ is the value of the visual features currently observed by the camera;
- C is a constant matrix which allows, for robustness issues, to take into account more visual features than necessary, and which will be fixed afterwards.

When stating the control problem as an output regulation problem, it appears that the concerned task is perfectly achieved if $e(t) = 0$. We may emphasize robustness issues with respect to model uncertainties by expressing this regulation problem as the problem of minimizing $\|e(t)\|$. Although all the theory was developed in a dynamical framework [8] with true joint torque control, we here assume for simplicity that the velocity ξ_c of the camera may be considered as a "control" vector. We thus may choose the following control law:

$$\xi_c = -\mu\ \underline{e}\ (t) \quad (3)$$

with $\mu > 0$. Indeed, if the object is motionless, we have:

$$\dot{\underline{e}} = C\dot{\underline{s}} = CL_{\underline{s}}^T \xi = -\mu\ CL_{\underline{s}}^T\ \underline{e} \quad (4)$$

An exponential convergence will thus be ensured under the sufficient condition:

$$CL_{\underline{s}}^T > 0 \quad (5)$$

in the sense that a $n \times n$ matrix A is positive if $x^T Ax > 0$ for any nonzero $x \in \mathbf{R}^n$.

A good and simple way to satisfy this convergence condition in the neighborhood of the desired position is to choose for the matrix C the pseudo inverse of the interaction matrix related to $\underline{s}^*$:

$$C = L^{T+}_{|\underline{s}=\underline{s}^*} \quad (6)$$

3 Modeling the Interaction Matrix

Espiau, et al [5] modeled a set of low level geometrical primitives such as points, lines, circles and spheres in the case of passive vision. In the present case of a *camera-light stripe* apparatus, the additional geometrical constraints introduced by the light stripe-camera coupling necessitate the modeling of the corresponding interaction matrices. In the past, we have constructed interaction matrices in a particular configuration between a polyhedral scene and a laser stripe [10]. Now, we present the modelisation in a general case for polyhedral and spherical scene.

3.1 Polyhedral scene:

3.1.1 Point Primitive: Intersection of a Laser Plane with Two Object Planes

The modeling is mainly based on the use of the 3D plane equations defined by the laser stripes and the polyhedral object surfaces (see Figure 1).

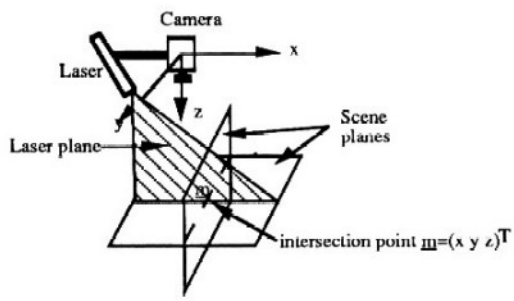

Figure 1: Intersection of a laser plane and two planes

The feature point is defined by the intersection of three planes:

- The plane P_l produced by a laser stripe rigidly attached to the camera reference frame:

$$P_l \ : \ ax + by + cz + d = 0 \quad (\text{with } a^2 + b^2 + c^2 = 1) \tag{7}$$

- two scene planes corresponding for example to the adjacent sides of a polyhedral object:

$$P_{obji} \ : \ a_i x + b_i y + c_i z + d_i = 0 \quad (\text{with } a_i^2 + b_i^2 + c_i^2 = 1) \text{ for } i = 1, 2 \tag{8}$$

If we only consider the case where the intersection of these three planes results in a point, the coordinates of the resulting point $\underline{m} = (x \ y \ z)^T$ are:

$$\underline{m} = -\mathbf{A}^{-1}\mathbf{B} \tag{9}$$

where $\mathbf{A} = \begin{pmatrix} a & b & c \\ a_1 & b_1 & c_1 \\ a_2 & b_2 & c_2 \end{pmatrix}$ and $\mathbf{B} = \begin{pmatrix} d \\ d_1 \\ d_2 \end{pmatrix}$.

Considering a pinhole camera with unit focal length, the point $\underline{m}$ in 3D space projects into $\underline{M} = (X \ Y \ 1)^T$ on the image frame with:

$$\underline{M} = \frac{1}{z}\underline{m} = \underline{\mathrm{F}}(\underline{\alpha}) \quad \text{with } \underline{\alpha} = (\alpha_1, \ldots, \alpha_{12}) = (a, b, c, d, a_1 \ldots, d_2) \tag{10}$$

We are interested in computing $\dot{\underline{M}}$. From (10), we immediately obtain:

$$\dot{\underline{M}} = \sum_{i=1}^{12} \frac{\partial \underline{M}}{\partial \alpha_i}\dot{\alpha}_i \tag{11}$$

The coefficients $\dot{\alpha}_i$ which represent the time variation of the planes induced by a motion of the object, may easily be obtained (let us note that $\dot{a}, \dot{b}, \dot{c}, \dot{d}$ are zero since the laser plane is rigidly attached to the camera frame). Indeed, if we consider a plane $P_i \ : \ a_i x + b_i y + c_i z + d_i = 0$ (with $a_i^2 + b_i^2 + c_i^2 = 1$) with motion $\xi = (\underline{T}, \underline{\Omega}) = (T_x, T_y, T_z, \Omega_x, \Omega_y, \Omega_z)$ where $\underline{T}$ and $\underline{\Omega}$ respectively represent the translational and rotational components of ξ, we have:

$$\begin{cases} a_i\dot{x} + b_i\dot{y} + c_i\dot{z} + \dot{a}_i x + \dot{b}_i y + \dot{c}_i z + \dot{d}_i = 0 \\ a_i\dot{a}_i + b_i\dot{b}_i + c_i\dot{c}_i = 0 \end{cases} \tag{12}$$

$$\text{with } \dot{\underline{m}} = \underline{T} + \underline{\Omega} \wedge \underline{m}, \forall \underline{m} \in P_i$$

Using three points belonging to the plane, we obtain a linear system, the solving gives:

$$\begin{cases} \dot{a}_1 = c_1\Omega_y - b_1\Omega_z \\ \dot{b}_1 = a_1\Omega_z - c_1\Omega_x \\ \dot{c}_1 = b_1\Omega_x - a_1\Omega_y \\ \dot{d}_1 = -(a_1 T_x + b_1 T_y + c_1 T_z) \end{cases} \tag{13}$$

This procedure is applied to each plane P_{obji} belonging to the object. Replacing equations (13) in (11) and simplifying the results using (10), the coupling matrix $L_{\underline{M}}^T = (L_X, L_Y)^T$ can be determined:

$$\dot{\underline{M}} = \begin{pmatrix} \dot{X} \\ \dot{Y} \end{pmatrix} = L_{\underline{M}}^T \cdot \xi \tag{14}$$

where:

$$L_X^T = \begin{pmatrix} \frac{(-(d_1b_2 - b_1d_2)a - \beta)\alpha}{\beta^2} \\ -\frac{b(d_1b_2 - b_1d_2)\alpha}{\beta^2} \\ \frac{(\beta X - c(d_1b_2 - b_1d_2))\alpha}{\beta^2} \\ \frac{\gamma_1}{\beta} - X\left(Y + \frac{c(d_1a_2 - a_1d_2)}{\beta}\right) \\ X\left(X - \frac{c(d_1b_2 - b_1d_2)}{\beta}\right) - \frac{(bd_2 - b_2d)a_1}{\beta} \\ \frac{(d_1b_2 - b_1d_2)(bX - aY)}{\beta} - Y \end{pmatrix}^T$$

$$L_Y^T - \begin{pmatrix} \frac{a(d_1a_2 - a_1d_2)\alpha}{\beta^2} \\ \frac{((d_1a_2 - a_1d_2)b - \beta)\alpha}{\beta^2} \\ \frac{(c(d_1a_2 - a_1d_2) + \beta Y)\alpha}{\beta^2} \\ -Y\left(Y + \frac{c(d_1a_2 - a_1d_2)}{\beta}\right) - \frac{(ad_2 - da_2)b_1}{\beta} \\ \frac{\gamma_2}{\beta} + Y\left(X - \frac{c(d_1b_2 - b_1d_2)}{\beta}\right) \\ \frac{(d_1a_2 - a_1d_2)(aY - bX)}{\beta} + X \end{pmatrix}^T \tag{15}$$

$$\text{with } \begin{cases} \alpha = & (c_1ba_2 - cb_1a_2 + cb_2a_1 \\ & +b_1c_2a - c_2ba_1 - b_2c_1a) \\ \beta = & (-ab_2d_1 + ab_1d_2 - ba_1d_2 \\ & +bd_1a_2 - db_1a_2 + db_2a_1) \\ \gamma_1 = & -db_1b_2 - cd_1c_2 + c_1cd_2 + b_1bd_2 \\ \gamma_2 = & -a_2a_1d + ad_2a_1 - cd_1c_2 + c_1cd_2 \end{cases}$$

3.1.2 Other Primitives:

By using two laser stripes, it can be interesting to introduce an other point of discontinuity : the intersection point between the two laser planes and one object plane. With the help of this primitive, the calculation procedure of the interaction matrix will be identical to the previous case, except that there is only one object plane in motion into the scene.

Moreover, with only one laser stripe, we can use the line primitive produced by the intersection of the laser plane with an object plane. The interaction matrix, using for example the line parameters ρ and θ ($X\cos\theta + Y\sin\theta - \rho - 0$), may be obtained in a similar manner.

3.2 Spherical scene:

We can use the same approach to perform positioning tasks on scenes containing spherical objects (see Figure 2). First of all, we have to select the features which will be used in the control scheme. Then, we have to compute the related interaction matrix:

The sphere is represented by its center $\underline{m_0} = (x_0\ y_0\ z_0)^T$ and its radius r, i.e:

$$(x - x_0)^2 + (y - y_0)^2 + (z - z_0)^2 - r^2 = 0 \quad (16)$$

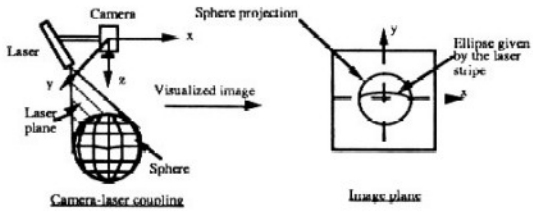

Figure 2: Camera-laser coupling with a sphere

An ellipse results from the projection in the image of the intersection between a sphere and a plane laser stripe (obviously, the camera only detects the portion of this ellipse corresponding to the sphere top side). The equation of this ellipse is given by :

$$g(\underline{X}, \underline{A}) = X^2 + A_1 Y^2 + 2A_2 XY + 2A_3 X + 2A_4 Y + A5 = 0 \quad (17)$$

$$\text{with} \begin{cases} \underline{X} = (X, Y) \\ \underline{A} = (A_1, \ldots, A_5) \end{cases}$$

where (see [3] for more details):

$$\begin{cases} A_1 = [b^2(z_0^2 + y_0^2 + x_0^2 - r^2) + 2bdy_0 + d^2]/A_0 \\ A_2 = [ab(z_0^2 + y_0^2 + x_0^2 - r^2) + ady_0 + bdx_0]/A_0 \\ A_3 = [ac(z_0^2 + y_0^2 + x_0^2 - r^2) + adz_0 + cdx_0]/A_0 \\ A_4 = [bc(z_0^2 + y_0^2 + x_0^2 - r^2) + bdz_0 + cdy_0]/A_0 \\ A_5 = [c^2(z_0^2 + y_0^2 + x_0^2 - r^2) + 2cdz_0 + d^2]/A_0 \end{cases} \quad (18)$$

with $A_0 = a^2(z_0^2 + y_0^2 + x_0^2 - r^2) + 2adx_0 + d^2 \neq 0$

Using the same approach as previously, we have:

$$\dot{\underline{A}} = \sum_{i=1}^{8} \frac{\partial \underline{A}}{\partial \alpha_i} \dot{\alpha}_i \text{ with } \alpha_i = (a, b, c, d, x_0, y_0, z_0, r) \quad (19)$$

In this case, $\dot{a} = \dot{b} = \dot{c} = \dot{d} = \dot{r} = 0$ and $\dot{\underline{m_0}} = \underline{T} + \Omega \wedge \underline{m_0}$ which allows to compute the interaction matrix $L_{\underline{A}}^T = (L_{A_1}, \ldots, L_{A_5})^T$ related to $\underline{A}$, with :

$$L_{A_1}^T = \frac{1}{A_0} \begin{pmatrix} 2b^2x_0 - 2A_1a^2x_0 - 2A_1ad \\ 2bd + 2b^2y_0 - 2A_1a^2y_0 \\ 2z_0(b^2 - A_1a^2) \\ -2bdz_0 \\ -2A_1adz_0 \\ 2d(A_1ay_0 + bx_0) \end{pmatrix}^T$$

$$L_{A_2}^T = \frac{1}{A_0} \begin{pmatrix} -2A_2a^2x_0 - 2A_2ad + 2abx_0 + bd \\ a(d + 2by_0 - 2A_2ay_0) \\ 2az_0(b - A_2a) \\ -adz_0 \\ dz_0(b - 2A_2a) \\ -d(by_0 - 2A_2ay_0 - ax_0) \end{pmatrix}^T$$

$$L_{A_3}^T = \frac{1}{A_0} \begin{pmatrix} -2A_3a^2x_0 - 2A_3ad + 2acx_0 + cd \\ 2ay_0(c - A_3a) \\ a(d + 2cz_0 - 2A_3az_0) \\ ady_0 \\ -d(2A_3az_0 + ax_0 - cz_0) \\ -dy_0(c - 2A_3a) \end{pmatrix}^T \quad (20)$$

$$L_{A_4}^T = \frac{1}{A_0} \begin{pmatrix} 2bcx_0 - 2A_4a^2x_0 - 2A_4ad \\ cd - 2A_4a^2y_0 + 2bcy_0 \\ bd + 2bcz_0 - 2A_4a^2z_0 \\ d(by_0 - cz_0) \\ -d(2A_4az_0 + bx_0) \\ d(cx_0 + 2A_4ay_0) \end{pmatrix}^T$$

$$L_{A_5}^T = \frac{1}{A_0} \begin{pmatrix} 2c^2x_0 - 2A_5a^2x_0 - 2A_5ad \\ 2y_0(c^2 - A_5a^2) \\ 2cd + 2c^2z_0 - 2A_5a^2z_0 \\ 2cdy_0 \\ -2d(A_5az_0 + cx_0) \\ 2A_5ady_0 \end{pmatrix}^T$$

4 Results and Analysis

4.1 Application: Positioning the End-Effector Tool Over a Vehicle Battery

The task is to position the camera with respect to a battery at a desired distance z^* (= 30cm), such that object plane and image plane will be parallel and such that the battery will be centered in the image (see Figure 3). In order to perform this task, we use two laser stripes coupled to the camera. Both laser planes are calibrated in order

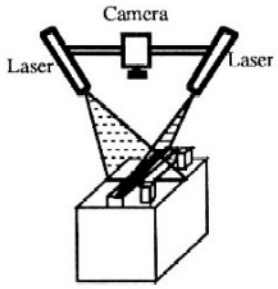

Figure 3: The sensory apparatus over a battery

to produce two orthogonal segments centered in the image at the desired position [10].

The elementary signals which will be used to perform this task are the coordinates of the four breakpoints produced by the two laser stripes : $\underline{s} = (X_1\ Y_1\ X_2\ Y_2\ X_3\ Y_3\ X_4\ Y_4)^T$ and we have, at the desired position (see Figure 4), $\underline{s}^\star = (X^\star\ 0\ -X^\star\ 0\ 0\ Y^\star\ 0\ -Y^\star)^T$ with $X^\star = L/2z^\star$ and $Y^\star = l/2z^\star$ where L and l are respectively the battery length and width.

The different planes used to compute the interaction matrix at the desired position are defined by:

Point 1 and 2:

- laser plane P_{l1} : $b_{l1}, c_{l1}, d_{l1} \neq 0$, but $a_{l1} = 0$ (laser plane parallel to X axis)
- object planes:
  1. $a_1 = 1,\ b_1 = 0,\ c_1 = 0,\ d_1 = \pm L/2$ (left and right planes of the battery).
  2. $a_2 = 0,\ b_2 = 0,\ c_2 = 1,\ d_2 = z^\star$ (top of the battery)

Point 3 and 4:

- laser plane P_{l2} : $a_{l2}, c_{l2}, d_{l2} \neq 0$, but $b_{l2} = 0$ (laser plane parallel to Y axis)
- object planes:
  1. $a_1 = 0,\ b_1 = 1,\ c_1 = 0,\ d_1 = \pm l/2$ (high and low edge of the battery)
  2. $a_2 = 0,\ b_2 = 0,\ c_2 = 1,\ d_2 = z^\star$ (top of the battery)

In this particular configuration, the expression of the interaction matrix is easily obtained from (15):

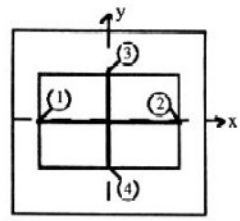

Figure 4: Image plane parallel to object plane, laser stripes with an orthogonal trace

$$L^T_{|\underline{s}=\underline{s}^\star} = \begin{pmatrix} 1/z^\star & 0 & -X^\star/z^\star \\ 0 & 0 & -c_{l1}/(z^\star b_{l1}) \\ 1/z^\star & 0 & X^\star/z^\star \\ 0 & 0 & -c_{l1}/(z^\star b_{l1}) \\ 0 & 0 & -c_{l2}/(z^\star a_{l2}) \\ 0 & 1/z^\star & -Y^\star/z^\star \\ 0 & 0 & -c_{l2}/(z^\star a_{l2}) \\ 0 & 1/z^\star & Y^\star/z^\star \end{pmatrix}$$

$$\begin{pmatrix} 0 & (X^{\star 2}+1) & 0 \\ 0 & (X^\star c_{l1})/b_{l1} & 0 \\ 0 & (X^{\star 2}+1) & 0 \\ 0 & -(X^\star c_{l1})/b_{l1} & 0 \\ -(Y^\star c_{l2})/a_{l2} & 0 & 0 \\ -(Y^{\star 2}+1) & 0 & 0 \\ (Y^\star c_{l2})/a_{l2} & 0 & 0 \\ -(Y^{\star 2}+1) & 0 & 0 \end{pmatrix} \quad (21)$$

We can note that this matrix is not of full rank because of the sixth column of $L^T_{|\underline{s}=\underline{s}^\star}$. This implies that the pseudo-inverse $C = L^{T\dagger}_{|\underline{s}=\underline{s}^\star}$, used in the task function (2), will have its last row equal to zero. In other terms, the rotational velocity Ω_z of the camera can not be controlled since its value, computed with the control scheme (3), will always be zero for all values of $\underline{s} - \underline{s}^\star$.

Furthermore, the geometry of our 5 d.o.f. manipulator doesn't provide the rotational velocity Ω_x so the experiment will be conducted in the case of a 4 d.o.f. to control. The coupling matrix $L^T_{|\underline{s}=\underline{s}^\star}$ will therefore be a 8×4 matrix and the combination matrix C its pseudo inverse.

Hereafter we present both simulation and experimental results obtained with the same initial positioning error in order to be compared. Let us note that the experiments have been conducted with a fictive battery with reduced dimensions (8cm*6cm) to be compatible with the

focal length of the camera (18mm). The different windows (see Figure 5) show simulation results in presence of noise (2% of white noise on the image coordinates and on the camera location) at the top and experimental results at the bottom. More precisely, from left to right, we present:

- the evolution of the light segments as seen by the camera (the edges of the battery are not detected by the camera),
- the behavior of each component of the control vector ξ_c during the visual servoing,
- the evolution of the error $\|e(t)\|$.

The convergence to the desired image target is performed and the behavior of the real system is extremely close to the one expected by the simulation. Note that the noise introduced on the measurements and on the robot locations brings little perturbation to the system. Experiments have been conducted on a great number of initial configurations and in all cases, in simulation as well as in the real experiment, the algorithm converged rapidly.

Let us now consider that the two laser stripes have some incline ($a_{l1} \neq 0$ and $b_{l2} \neq 0$). The interaction matrix thus becomes of full rank and we can control the 6 d.o.f. of the camera to perform the same task. The corresponding simulation results are presented on the Figure 6.

4.2 Positioning with respect to a sphere

The task is to position the camera with respect to a sphere such that its projection in the image gives a centered circle ($x_0 = y_0 = 0, z_0 = z^\star$). Using again two orthogonal laser stripes ($a_{l1} = b_{l2} = 0$), we can choose $s = (A_{11}\ A_{21}\ A_{31}\ A_{41}\ A_{51}\ A_{12}\ A_{22}\ A_{32}\ A_{42}\ A_{52})$ where A_{ij} is the parameter A_i corresponding to the ellipse j. At the desired position, we can compute $\underline{s}^\star$ using (18): $s^\star = (A^\star_{11}\ A^\star_{21}\ A^\star_{31}\ A^\star_{41}\ A^\star_{51}\ A^\star_{12}\ A^\star_{22}\ A^\star_{32}\ A^\star_{42}\ A^\star_{52})$ with:

$$\begin{cases} A^\star_{11} = [b^2_{l1}(z^\star - r^2) + d^2_{l1}]/A^\star_{01} \\ A^\star_{21} = 0 \\ A^\star_{31} = 0 \\ A^\star_{41} = [b_{l1}c_{l1}(z^\star - r^2) + b_{l1}d_{l1}z^\star]/A^\star_{01} \\ A^\star_{51} = [c^2_{l1}(z^\star - r^2) + 2c_{l1}d_{l1}z^\star + d^2_{l1}]/A^\star_{01} \\ A^\star_{01} = d^2_{l1} \end{cases} \tag{22}$$

$$\begin{cases} A^\star_{12} = d^2_{l2}/A^\star_{02} \\ A^\star_{22} = 0 \\ A^\star_{32} = [a_{l2}c_{l2}(z^\star - r^2) + a_{l2}d_{l2}z^\star]/A^\star_{02} \\ A^\star_{42} = 0 \\ A^\star_{52} = [c^2_{l2}(z^\star - r^2) + 2c_{l2}d_{l2}z^\star + d^2_{l2}]/A^\star_{02} \\ A^\star_{02} = a^2_{l2}(z^\star - r^2) + d^2_{l2} \end{cases} \tag{23}$$

The interaction matrix related to $\underline{s} = \underline{s}^\star$ is obtained from (20):

$$L^T_{|\underline{s}=\underline{s}^\star} = \begin{pmatrix} 0 & \frac{2b_1d_1}{A^\star_{01}} \\ 0 & 0 \\ 0 & 0 \\ \frac{c_1d_1}{A^\star_{01}} & \frac{b_1(2c_1z^\star+d_1)}{A^\star_{01}} \\ 0 & \frac{2c_1(c_1z^\star+d_1)}{A^\star_{01}} \\ 0 & \frac{-2A^\star_{12}a^2_2z^\star}{A^\star_{02}} \\ \frac{a_2d_2}{A^\star_{02}} & 0 \\ 0 & \frac{-a_2(-2c_2z^\star-d_2+2A^\star_{32}a_2z^\star)}{A^\star_{02}} \\ \frac{c_2d_2}{A^\star_{02}} & 0 \\ 0 & \frac{2c^2_2z^\star+2c_2d_2-2A^\star_{52}a^2_2z^\star}{A^\star_{02}} \end{pmatrix}$$

$$\begin{pmatrix} \frac{2b^2_1z^\star}{A^\star_{01}} & \frac{-2b_1d_1z^\star}{A^\star_{01}} & 0 & 0 \\ \frac{b_1d_1}{A^\star_{01}} & 0 & \frac{b_1d_1z^\star}{A^\star_{01}} & 0 \\ \frac{c_1d_1}{A^\star_{01}} & 0 & \frac{c_1d_1z^\star}{A^\star_{01}} & 0 \\ 0 & \frac{-c_1d_1z^\star}{A^\star_{01}} & 0 & 0 \\ 0 & 0 & 0 & 0 \\ \frac{-2A^\star_{12}a_2d_2}{A^\star_{02}} & 0 & \frac{-2A^\star_{12}a_2d_2z^\star}{A^\star_{02}} & 0 \\ 0 & \frac{-a_2d_2z^\star}{A^\star_{02}} & 0 & 0 \\ \frac{-d_2(2A^\star_{32}a_2-c_2)}{A^\star_{02}} & 0 & \frac{-d_2z^\star(2A^\star_{32}a_2-c_2)}{A^\star_{02}} & 0 \\ 0 & \frac{-c_2d_2z^\star}{A^\star_{02}} & 0 & 0 \\ \frac{-2A^\star_{52}a_2d_2}{A^\star_{02}} & 0 & \frac{-2A^\star_{52}a_2d_2z^\star}{A^\star_{02}} & 0 \end{pmatrix} \tag{24}$$

In this case, the rank of $L^T_{|\underline{s}=\underline{s}^\star}$ is 3. To perform this task, we have used in the control scheme the translational velocities V_x, V_y and V_z of the camera. We present simulation results on the Figure 7, with a noise corresponding to the ellipse parameter error owing to the image processing. Let us note that, because of the particular configuration of $L^T_{|\underline{s}=\underline{s}^\star}$, Ω_y could be used instead of V_x and Ω_x instead of V_y.

5 Concluding Remarks

The interest of this visual servoing approach is that the intermediary step of 3D recovery of the object position and motion, with regard to the camera location, is suppressed by using directly

image signals as errors to input in a robust control scheme. Using a camera-light stripe coupling as sensor in a robotics control scheme enabled the real time implementation on a low-cost system.

When this specific coupling is projected onto polyhedral and spherical scenes, we have defined various *interaction matrices*. The robustness and stability of the control scheme has been proved in several simulation testing and in a real experiment built in our laboratory.

References

[1] G.J. Agin: *Real-time control of a robot with a mobile camera*, 9th Int. Symp. on Industrial Robots, Washington D.C., pp. 233-246, 1979.

[2] G.J. Agin: *Calibration and use of a light stripe range sensor mounted on the hand of a robot*, IEEE Int. Conference on Robotics and Automation, St-Louis, March, 1985.

[3] F. Chaumette: *La relation vision-commande : théorie et application à des tâches robotiques*, PhD Thesis, Rennes, France, July 1990.

[4] B. Espiau, C. Samson : *Sensory based control. Robustness issues and modeling technics. Application to proximity sensing*, NATO Workshop on Kinematic and dynamic Issues in Sensor Based Control, Pisa, 1987.

[5] B. Espiau, F. Chaumette, P. Rives: *A new approach to visual servoing in robotics*, Trans. on Robotics and Automation, Vol. 8, n. 3, June 1992.

[6] J. T. Feddema, O. R. Mitchell: *Vision-Guided Servoing with Feature - Based Trajectory Generation*, IEEE Trans. on Robotics and Automation, Vol. 5, n. 5, October 1989.

[7] A.L. Gilbert, M.K. Giles, G.M. Fachs, R.B. Rogers, Y.Hsun: *A real-time video tracking system*, IEEE Trans. on Pattern Analysis and Machine Intelligence, Vol. PAMI-2, n. 1, pp. 47-56, 1980.

[8] C. Samson, M. Le Borgne, B. Espiau: *Robot Control: The Task Function Approach*, Oxford University Press, 1991.

[9] A.C. Sanderson, L. Weiss: *Adaptive Visual Servo Control of Robots*, In Pugh A. (editor), Robot Vision, I.F.S. Publications Ltd., pp. 107-116, 1983.

[10] J.P. Urban, G. Motyl, J. Gallice: *A Visual Servoing Approach Applied to Robotic Tasks*, IAPR Workshop on Machine Vision Applications, Tokyo, Japan, pp. 351 355, November 1990.

[11] L. E. Weiss, A. C. Sanderson: *Dynamic Sensor-Based Control of Robots with Visual Feedback*, IEEE Journal of Robotics and Automation, Vol. RA-3, n. 5, pp. 404-417

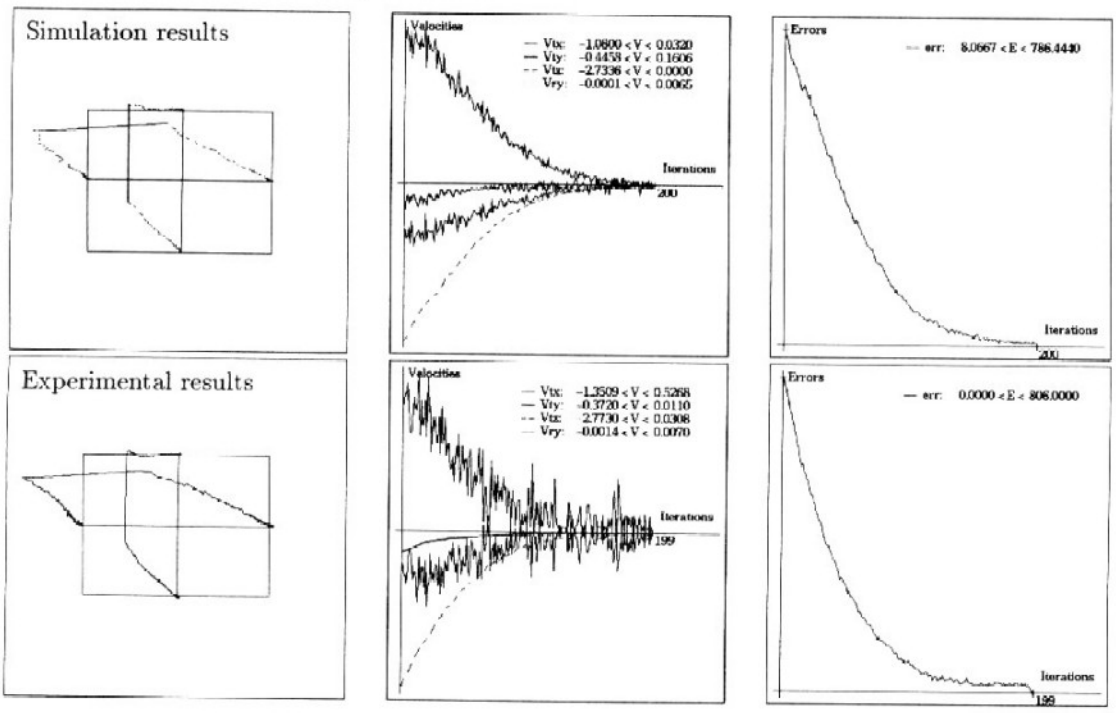

Figure 5: Positioning in front of a battery using two orthogonal laser stripes

(simulation with noise and experimental results)

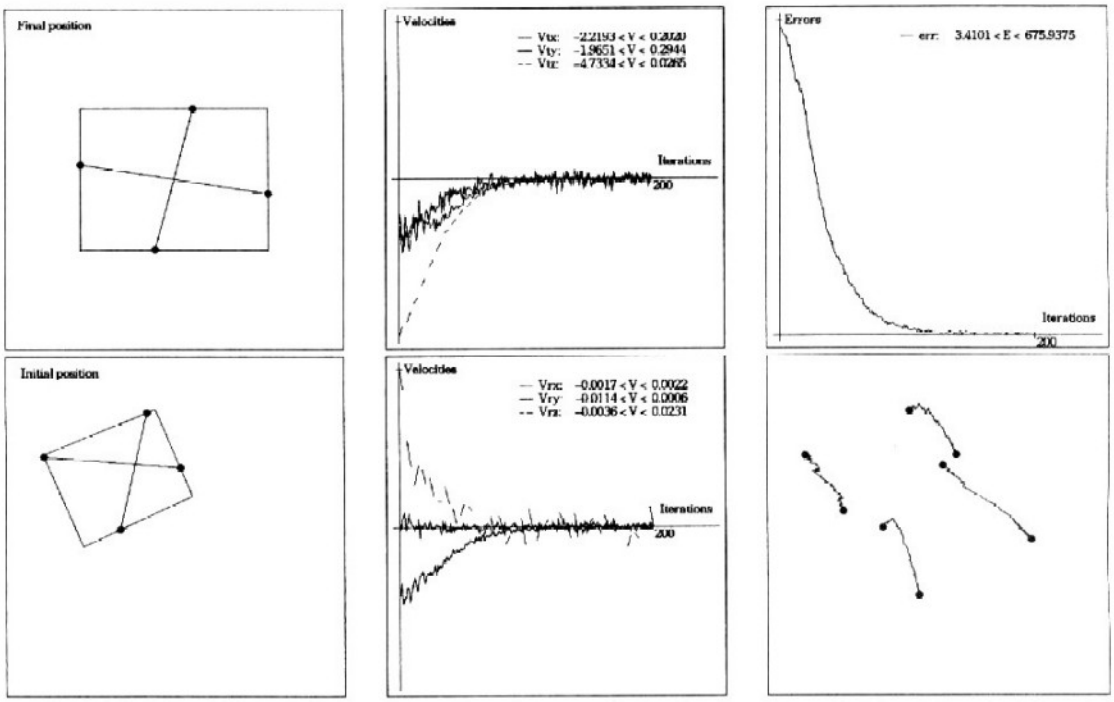

Figure 6: Positioning in front of a battery using two incline laser stripes

(simulation with noise)

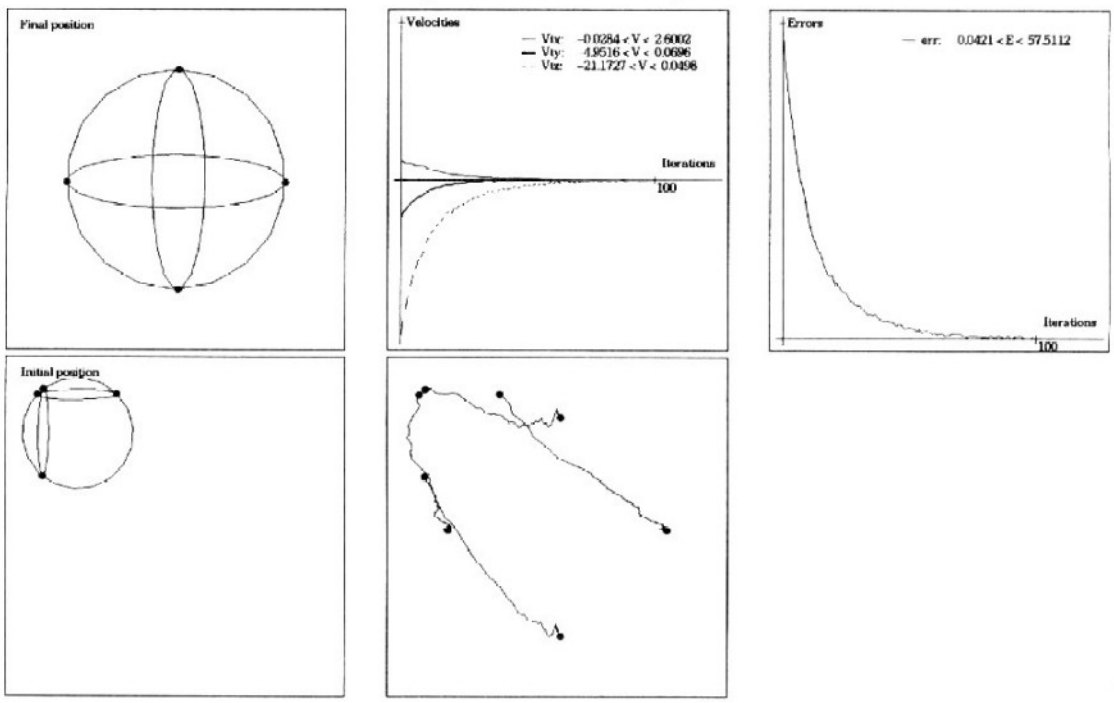

Figure 7: Positioning with respect to a sphere

(simulation with noise)